Influence of thermal growth parameters on the SiO2/4H-SiC interfacial region

E. Pitthan, L. D. Lopes, R. Palmieri, S. A. Corrêa, G. V. Soares, H. I. Boudinov, and F. C. Stedile

Citation: APL Mater. **1**, 022101 (2013); doi: 10.1063/1.4817896
View online: http://dx.doi.org/10.1063/1.4817896
View Table of Contents: http://scitation.aip.org/content/aip/journal/aplmater/1/2?ver=pdfcov
Published by the AIP Publishing

Articles you may be interested in

Influence of CO annealing in metal-oxide-semiconductor capacitors with SiO2 films thermally grown on Si and on SiC
J. Appl. Phys. **119**, 025307 (2016); 10.1063/1.4939836

Cathodoluminescence study of radiative interface defects in thermally grown SiO2/4H-SiC(0001) structures
Appl. Phys. Lett. **106**, 261604 (2015); 10.1063/1.4923470

Fabrication of SiO2/4H-SiC (0001) interface with nearly ideal capacitance-voltage characteristics by thermal oxidation
Appl. Phys. Lett. **105**, 032106 (2014); 10.1063/1.4891166

Effects of sodium ions on trapping and transport of electrons at the SiO2/4H-SiC interface
J. Appl. Phys. **115**, 034502 (2014); 10.1063/1.4861646

Investigation of unusual mobile ion effects in thermally grown SiO2 on 4H-SiC(0001) at high temperatures
Appl. Phys. Lett. **100**, 252103 (2012); 10.1063/1.4729780

AIP Applied Physics Reviews
NEW Special Topic Sections
NOW ONLINE
Lithium Niobate Properties and Applications: Reviews of Emerging Trends
AIP Applied Physics Reviews

Reuse of AIP Publishing content is subject to the terms at: https://publishing.aip.org/authors/rights-and-permissions. Download to IP: 200.130.19.173 On: Wed, 20 Apr 2016 19:01:00

APL MATERIALS **1**, 022101 (2013)

Influence of thermal growth parameters on the SiO_2/4H-SiC interfacial region

E. Pitthan,[1,a] L. D. Lopes,[2] R. Palmieri,[3] S. A. Corrêa,[1] G. V. Soares,[1,3] H. I. Boudinov,[1,3] and F. C. Stedile[1,2]
[1]*PGMICRO, Universidade Federal do Rio Grande do Sul, 91509-900 Porto Alegre, RS, Brazil*
[2]*Instituto de Química, Universidade Federal do Rio Grande do Sul, 91509-900 Porto Alegre, RS, Brazil*
[3]*Instituto de Física, Universidade Federal do Rio Grande do Sul, 91509-900 Porto Alegre, RS, Brazil*

(Received 8 February 2013; accepted 15 May 2013; published online 9 August 2013)

In order to elucidate the origin of SiC electrical degradation from thermal oxidation, 4H-SiC substrates were thermally oxidized under different conditions of time and pressure. Results from nuclear reaction analyses were correlated to those from electrical measurements. Although the increase in the flatband voltage shift and in the film thickness were related to the oxidation parameters, the results exclude the thickness of the SiO_2/4H-SiC interfacial region and the amount of residual oxygen compounds present on the SiC surface as the main cause of the electrical degradation from the SiC oxidation. © *2013 Author(s). All article content, except where otherwise noted, is licensed under a Creative Commons Attribution 3.0 Unported License.* [http://dx.doi.org/10.1063/1.4817896]

Silicon carbide (SiC) is a promising semiconductor to replace Si in micro and nanoelectronics device applications that require high-power, high-frequency, and/or high-temperature.[1,2] Besides, a SiO_2 film can be thermally grown in a similar way to that on Si, allowing the technology used to produce MOS (metal-oxide-semiconductor) devices to be adapted to the case of SiC.[3] Nevertheless, the oxidation of SiC leads to a higher interface states density (D_{it}) in the SiO_2/SiC interface as compared to the Si case.[1] Although successful routes to reduce D_{it} were achieved, like thermal treatments involving NO, N_2O, and H_2,[4–6] the nature of the defects responsible for the electrical degradation in the SiO_2/SiC interfacial region is not yet completely understood.

Concerning SiC oxidation, excess of carbon near the formed interfacial region was observed by different techniques,[7–10] although medium energy ion scattering (MEIS) analysis indicates a stoichiometric SiO_2 film formed from the SiC oxidation.[11] Besides, a non abrupt interface between SiO_2 films and SiC was revealed by nuclear reaction profiling (NRP)[12–14] differently from the case of silicon oxidation.[12,15] The probable causes for the presence of these interfacial regions can be: roughness,[13,16] oxygen vacancies,[17] or even excess of carbon.[7–10] Moreover, residual compounds on the SiC surface after the removal of the oxide film were observed.[18–20] Such compounds exhibit different properties when using Si or C face terminated substrates.[20] These compounds were not observed in the silicon case,[19] being probably related to the presence of silicon bonded to oxygen and to carbon in different stoichiometries, named silicon oxycarbides (SiC_xO_y).[21,22] Many trials to remove these compounds in wet environments were unsuccessful evidencing their high chemical resistance.[19] However, the use of a flux of O_2 bubbled in hot H_2O_2 proved to be efficient in removing partially these SiC_xO_y,[23] reducing D_{it} in the SiO_2/4H-SiC and decreasing the interfacial thickness after further reoxidation steps.[14] In order to elucidate how these residual compounds and how the SiO_2/4H-SiC interfacial region thickness determined by NRP influence the electrical properties of the SiC MOS structures, more investigations must be performed. In this work, we propose to

[a]Electronic mail: eduardo.pitthan@ufrgs.br

 ©Author(s) 2013

Reuse of AIP Publishing content is subject to the terms at: https://publishing.aip.org/authors/rights-and-permissions. Download to IP: 200.130.19.173 On: Wed, 20 Apr 2016 19:01:00

investigate the relation between these characteristics obtained by nuclear reaction analyses and the modification in the electrical properties induced by the thermal growth parameters oxidation time and oxygen pressure. Thus, we expect to achieve a better understanding on the SiC thermal oxidation and on the origin of the electrical defects present in the SiO_2/SiC interfacial region.

To achieve these goals, different subatmospheric oxygen pressures (of $^{18}O_2$) and oxidation times were used to thermally grow thin SiO_2 films on 4H-SiC substrates. Samples were probed by nuclear reaction analysis (NRA) to determine the total amount of oxygen incorporated before and after the removal of the $Si^{18}O_2$ film, and by NRP to determine its depth distribution. Current-voltage (I-V) and capacitance-voltage (C-V) measurements were performed in Al/SiO_2/4H-SiC MOS structures and correlated with the other results.

Commercial SiC wafers of the 4H polytype, polished in both (0001) and (000$\underline{1}$) faces (terminated in Si and C, respectively), were employed as substrates. Samples characterized by electrical measurements were 4H-SiC (n-type) commercial epitaxial wafers, 8° off-axis on the Si face, doped with nitrogen (1.1×10^{16} cm^{-3}), 4.6 μm thick. Wafers were purchased from CREE Inc. Research. All substrates were cleaned in a mixture of H_2SO_4 and H_2O_2 followed by the standard RCA (Radio Corporation of America) process.[24] Then samples were etched for 60 s in a 1 vol.% aqueous solution of hydrofluoric acid (40 wt.% HF, purchased from Merck) and rinsed in deionized water. Immediately after blow drying with N_2, 4H-SiC samples were loaded in a static pressure, quartz tube, resistively heated furnace that was pumped down to 10^{-7} mbar. SiO_2 films were thermally grown at 1100 °C in different oxygen pressures (50, 100, and 200 mbar) and oxidation times (0.5, 1, 2, 3, and 4 h) of dry O_2 (<1 ppm H_2O) enriched to 97% in the ^{18}O isotope, whose natural abundance is 0.2%, named $^{18}O_2$. Oxygen pressures higher than 200 mbar were not employed in this work due to the use of a N_2(L) trap to help the base pressure reduction (mainly H_2O molecules condensation) while keeping O_2 molecules in the gas phase, which would condensate at higher pressures. The use of ^{18}O is crucial, as the used nuclear reaction analyses allow to distinguish it from oxygen eventually incorporated from other sources (for instance, from exposure to the ambient). The total amount of ^{18}O in resulting samples was determined by NRA using the $^{18}O(p,\alpha)^{15}N$ nuclear reaction at 730 keV,[25] referenced to a standard $Si^{18}O_2$ film on Si.[26] The depth distribution of ^{18}O in the samples was determined by NRP using the narrow resonance at 151 keV in the cross section curve of the $^{18}O(p,\alpha)^{15}N$ nuclear reaction. ^{18}O concentration profiles were determined from experimental excitation curves (alpha particle yield versus incident proton energy)[27] using the FLATUS code. With the experimental condition used in this work, a sub-nanometric resolution can be obtained near the surface. Al thermal evaporation to obtain MOS structures used a mechanical mask, forming circular capacitors with a diameter of 200 μm. An InGa eutectic was used as back contact. Samples were electrically characterized using a computer-controlled HP4155A Semiconductor Parameter Analyzer for the I-V curves. The C-V curves were taken from inversion to accumulation at 100 kHz with a 0.25 V/s rate using a HP4284A Precision *LCR* Meter.

The total amount of ^{18}O and the corresponding $Si^{18}O_2$ film thickness of the SiC samples before etching are presented in top panel of Figure 1. These results are presented as a function of the product of pressure and time (p × t). The motivation for such plot was that for the Si and for the SiC oxidations, despite being valid for a different thickness range (films thicker then ∼25 nm[28,29]), a given SiO_2 film thickness can be reached by maintaining the product of oxygen pressure and time constant. For the SiC case, the p × t dependence was investigated for oxygen pressures higher than those of the present work, presenting deviation from this behavior for pressures higher than 1 atm in the case of Si face samples. In the present samples, whose thicknesses are in the 3–8 nm interval for the Si face and 7–24 nm for the C face, a linear behavior of the amount of incorporated ^{18}O can be observed in both faces, although it was expected a more rapid oxide growth rate up to ∼10 nm for both Si and SiC oxidations.[30,31] It is possible to convert the ^{18}O amount into oxide film thickness by assuming a given density to the oxide film. In the present case, it was assumed 2.21 g/cm^3, typical of silicon dioxide films thermally grown on Si. However, this conversion might not be accurate due to modifications in the oxide density in the initial oxidation steps.[32] Nevertheless, what is being highlighted from these results is that the linear dependence of the ^{18}O incorporated amount in the silicon oxide films on (p × t) is still valid for the thermal oxidation conditions tested for both Si and C faces of SiC. It means that for the initial stages of oxidation, this relation between oxygen pressure

Reuse of AIP Publishing content is subject to the terms at: https://publishing.aip.org/authors/rights-and-permissions. Download to IP: 200.130.19.173 On: Wed, 20 Apr 2016 19:01:00

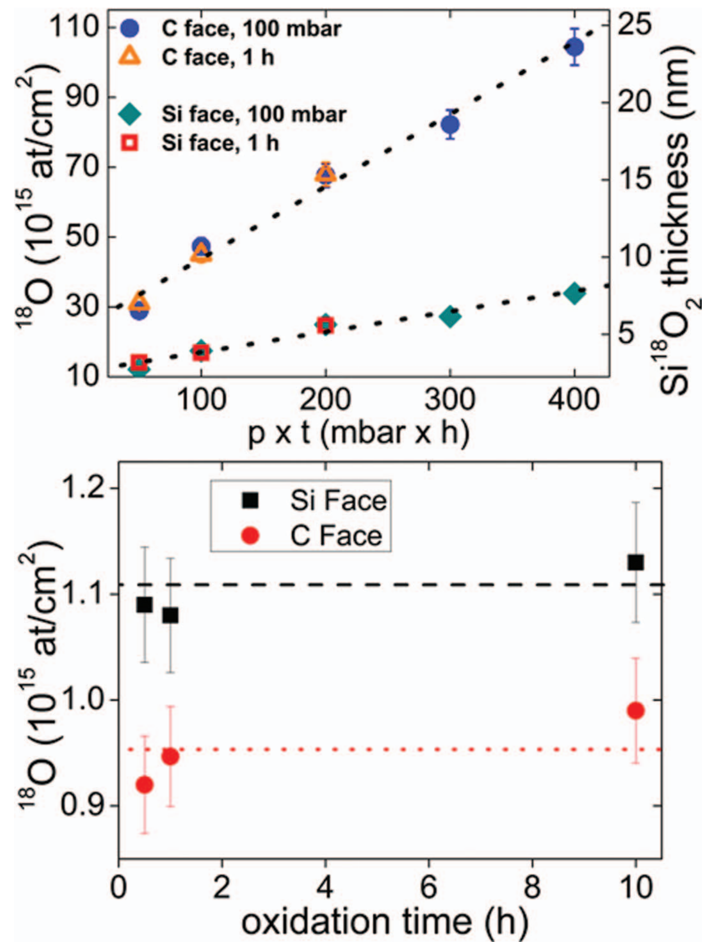

FIG. 1. (Top) ^{18}O amounts obtained by NRA from samples submitted to different oxidation times (0.5, 1, 2, 3, and 4 h) and oxygen pressures (50, 100, and 200 mbar) at 1100 °C on 4H-SiC on both Si and C faces. Film thicknesses were calculated assuming that the SiO_2 density on SiC is 2.21 g cm^{-3}. (Bottom) Amount of residual ^{18}O after etching in aqueous HF of samples oxidized at 1100 °C and 100 mbar of $^{18}O_2$ under different oxidation time conditions. Error bars correspond to experimental accuracy of 5%.

and oxidation time can be used to determine the SiO_2 film thickness on SiC. The residual amount of ^{18}O after etching in aqueous HF as a function of oxidation time is presented in bottom panel of Figure 1 for samples synthesized under different time oxidation conditions. As already observed,[20] the Si face presents higher residual oxygen amounts than the C face. However, in present results no relation was observed with oxidation time, indicating that the amount of residual compounds is not affected by the oxidation parameter tested.

Figures 2(a) and 2(b) show the excitation curves of the $^{18}O(p,\alpha)^{15}N$ nuclear reaction and the ^{18}O concentration profiles obtained for 4H-SiC samples submitted to different $^{18}O_2$ pressures and oxidation times at 1100 °C. The horizontal lines at 97% observed in Figure 2 profiles refer to a stoichiometric $Si^{18}O_2$ film, while the decrease in the ^{18}O concentration towards zero refers to its concentration in the SiO_2/4H-SiC interfacial region. Interfacial region thicknesses around 3 nm (considering the thickness interval from when the ^{18}O concentration starts to decrease until when this concentration is negligible) can be observed for all C-face oxidized samples, in good agreement with our previous results.[13,14] For Si-face oxidized samples, only the sample oxidized under 50 mbar presented a thicker interfacial region (around 3.8 nm). The decrease in the thickness of the SiO_2/SiC transition layer as the oxide film thickness is increased during the initial stages of oxidation can be attributed to a smoothing effect of the interface, as suggested by Szilágyi *et al.*[32] Thus, no significant

Reuse of AIP Publishing content is subject to the terms at: https://publishing.aip.org/authors/rights-and-permissions. Download to IP: 200.130.19.173 On: Wed, 20 Apr 2016 19:01:00

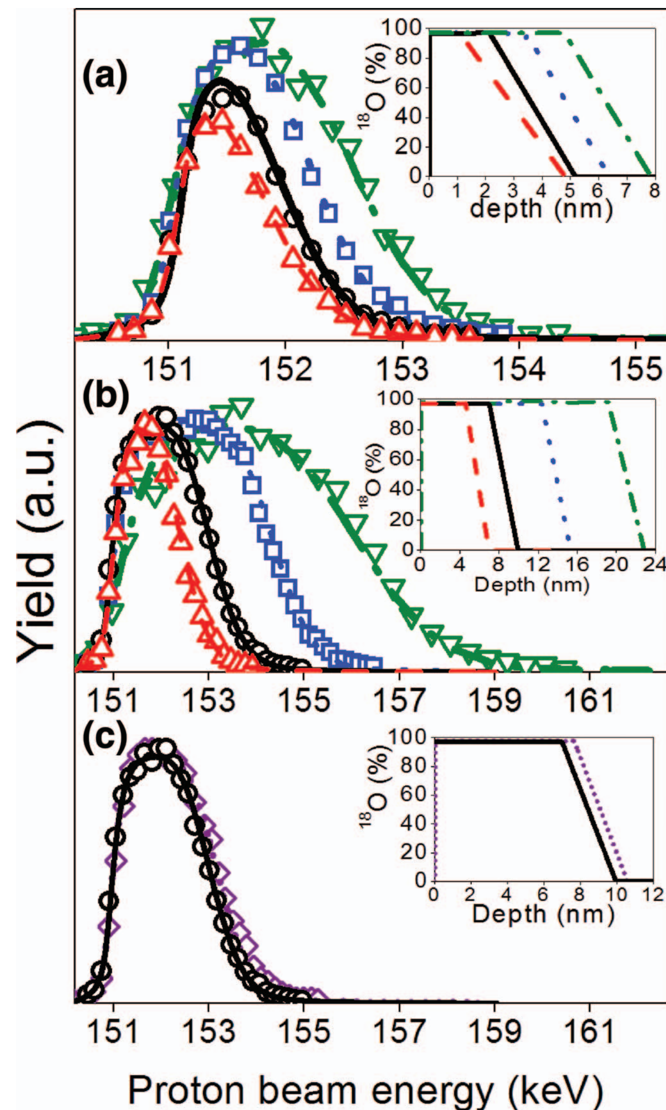

FIG. 2. Experimental (symbols) excitation curves of the $^{18}O(p,\alpha)^{15}N$ nuclear reaction around the resonance at 151 keV and the corresponding simulations (lines) for 4H-SiC samples oxidized for 1 h in 50 (triangle and dashed line), 100 (circle and solid line), and 200 mbar (square and dotted line) of $^{18}O_2$, and for 3 h at 100 mbar (inverted triangle, dotted/dashed line) at 1100 °C. (a) For the Si-face and (b) for C-face samples. (c) Excitation curves and the corresponding simulations for the same nuclear reaction for a 4H-SiC (C-face) sample oxidized for 10 h in 100 mbar of $^{18}O_2$ at 1100 °C followed by aqueous etching in HF for 290 s (diamond and short dotted line) and of a 4H-SiC (C-face) sample oxidized for 1 h in 100 mbar of $^{18}O_2$ at 1100 °C (circle and solid line). Insets: ^{18}O profiles obtained from the simulation of excitation curves using the same line types.

modifications in the SiO_2/SiC interfacial region thickness attributable to the oxygen pressure and oxidation time were observed.

To investigate the SiO_2/SiC interfacial region thickness in conditions of a longer oxidation time, a sample was oxidized for 10 h in 100 mbar of $^{18}O_2$ at 1100 °C. To avoid a degradation of depth resolution around the interfacial region due to the thicker film, the upper part of the film was partially removed with a controlled etching[19] for 290 s. In this way, the final film thickness was almost the same of the sample oxidized for 1 h, simplifying the comparison. The excitation curve of the $^{18}O(p,\alpha)^{15}N$ nuclear reaction and the ^{18}O concentration profile on the C-face are presented and compared to a sample oxidized for 1 h in 100 mbar of $^{18}O_2$ at 1100 °C in Figure 2(c). Again,

Reuse of AIP Publishing content is subject to the terms at: https://publishing.aip.org/authors/rights-and-permissions. Download to IP: 200.130.19.173 On: Wed, 20 Apr 2016 19:01:00

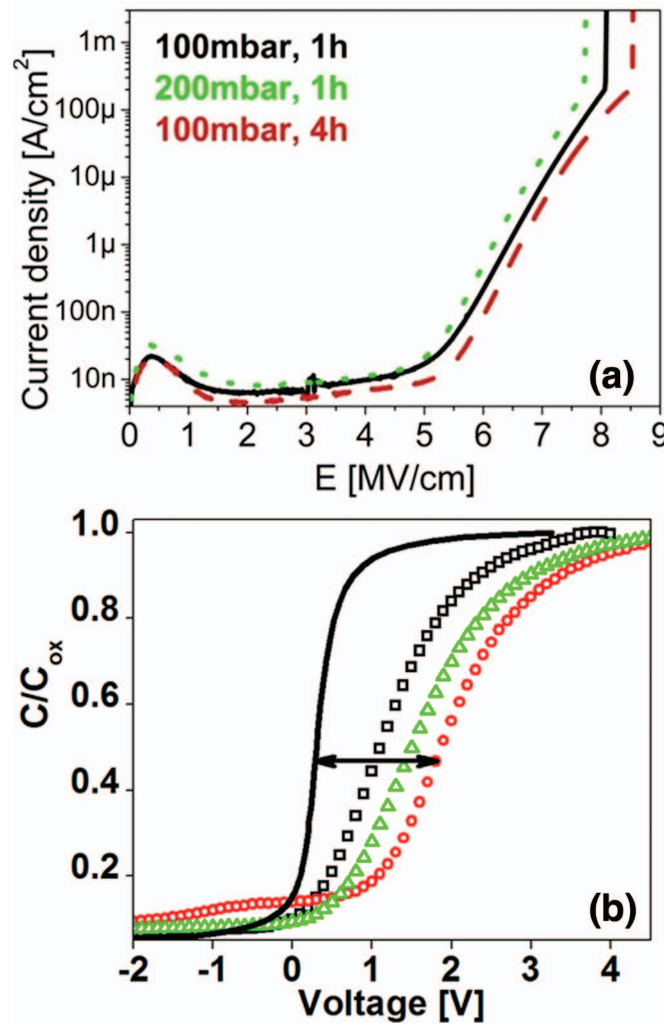

FIG. 3. (a) I-V curves and (b) C-V curves (open symbols are experimental data and line is the ideal curve. The arrow indicates where V_{fb} was extracted for the sample oxidized for 4 h. For the other samples, it is not shown since it is alike) of Al/SiO_2/4H-SiC structures. Oxygen pressure and oxidation time are indicated. Oxidation temperature was 1100 °C for all samples.

no major modification was observed in the SiO_2/SiC interfacial region thickness, confirming the absence of influence of the oxidation time in this property.

I-V and C-V curves for samples oxidized at 1100 °C for 1 h in 100 mbar, 1 h in 200 mbar, and 4 h in 100 mbar are presented in Figure 3, and their results are summarized in Table I. The I-V curves presented breakdown fields around 8.0 MV/cm, almost independent of the oxidation parameters, indicating minor modifications in the nature of the SiO_2 from the oxidation conditions tested. C-V curves indicate that the increase of the flatband voltage (V_{fb}) follows the p × t behavior, and the increase of both oxidation parameters induced a higher effective charge concentration, although not in the same proportion, with oxygen pressure being more important than oxidation time in inducing the highest effective charge concentration. Nevertheless, this is considered an important finding, since the presence of effective negative fixed charge plays a major role in the effective mobility of SiC based MOSFETs.[33] These results reveal that a higher oxygen pressure also induces a larger electrical degradation, similar to the well-known effect of longer oxidation times.[34,35] Thus, the electrical degradation seems to be controlled by the p × t parameter, i.e., an oxidation parameter that accelerates the SiO_2 film growth should lead to a larger electrical degradation. Therefore, alternative ways to obtain SiO_2 films on SiC such as thermal growing of a very thin and stoichiometric SiO_2 film

Reuse of AIP Publishing content is subject to the terms at: https://publishing.aip.org/authors/rights-and-permissions. Download to IP: 200.130.19.173 On: Wed, 20 Apr 2016 19:01:00

TABLE I. Electrical parameters obtained from C-V and I-V measurements for Al/SiO_2/4H-SiC Si face, n-type structures.

Oxidation conditions	V_{fb} (V)	Q_{eff} ($\times 10^{12}$ cm^{-2})	E_{max} (MV/cm)
100 mbar, 1 h, 1100 °C	0.9	−2.0	8.0
200 mbar, 1 h, 1100 °C	1.4	−3.3	7.7
100 mbar, 4 h, 1100 °C	1.9	−2.7	8.5

in a minimal oxidation condition followed by the SiO_2 film deposition,[36] or the oxidation of a Si/SiC heterojunction produced by a layer-transfer process,[37] or even the direct deposition of the SiO_2 film on the SiC substrate, reducing the influence of the substrate in the thermal oxide formation[38] should be investigated in order to minimize the formation of electrical active defects in the SiO_2/SiC structure.

Results presented in this work exclude the thickness of the SiO_2/4H-SiC interfacial region and the amount of residual compounds present on the SiC surface as the main cause of the electrical degradation originated from SiC thermal oxidation. Concerning the presence of effective negative fixed charge observed in our electrical measurements, Ebihara and co-workers[39] recently attributed the presence of negative fixed charge to be from CO_3-like moiety formed from the interaction of the SiO_2 film with residual carbon atoms. Therefore, a possible explanation for the origin of the electrical degradation caused by SiC thermal oxidation is the interaction of the oxidation by-products with the SiO_2 bulk.[10] By-products formed in this work would contain ^{18}O and can be incorporated in the solid phase in all depth regions of the film. When submitting the film to HF etching, the only compounds that remain in the sample are those insoluble in the previous near-interface region. Thus, the fact that no modification in the amount of residual compounds was observed after the removal of the oxide film in HF corroborates this hypothesis.

In summary, this work presented the influence in the electrical and structural properties of low oxygen pressures and different times of thermal oxidation of 4H-SiC on both Si and C faces. Although the product oxygen pressure with oxidation time controlled the total amount of oxygen incorporated in both faces, it does not affect the amount of residual compounds after etching the sample in HF or the SiO_2/4H-SiC interfacial region thickness. On the other hand, the V_{fb} was influenced by those parameters inducing higher negative effective charge concentrations, indicating that increasing oxygen pressure during thermal oxidation can induce an electrical degradation in a similar way to oxidation time. The possibility that the origin of this electrical degradation is in the interaction of SiC oxidation by-products with the SiO_2 bulk should not be disregarded.

The authors would like to thank INCTs Namitec and INES, MCT/CNPq, INCT, CAPES, and FAPERGS for financial support.

[1] J. B. Casady and R. W. Johnson, Solid-State Electron. **39**, 1409 (1996).
[2] V. Presser and K. G. Nickel, Crit. Rev. Solid State Mater. Sci. **33**, 1 (2008).
[3] W. Wesch, Nucl. Instrum. Methods Phys. Res. B **116**, 305 (1996).
[4] V. V. Afanas'ev, A. Stesmans, F. Ciobanu, G. Pensl, K. Y. Cheong, and S. Dimitrijev, Appl. Phys. Lett. **82**, 568 (2003).
[5] S. Dhar, S. Wang, J. R. Williams, S. T. Pantelides, and L. C. Feldman, MRS Bull. **30**, 288 (2005).
[6] S. Wang, S. Dhar, S. Wang, A. C. Ahyi, A. Franceschetti, J. R. Williams, L. C. Feldman, and S. T. Pantelides, Phys. Rev. Lett. **98**, 026101 (2007).
[7] K. C. Chang, N. T. Nuhfer, L. M. Porter, Q. Wahab, Appl. Phys. Lett. **77**, 2186 (2000).
[8] K.-C. Chang, L. M. Porter, J. Bentley, C.-Y. Lu, and J. Cooper, Jr., J. Appl. Phys. **95**, 8252 (2004).
[9] T. Zheleva, A. Lelis, G. Duscher, F. Liu, I. Levin, and M. Das, Appl. Phys. Lett. **93**, 022108 (2008).
[10] C. Radtke, F. C. Stedile, G. V. Soares, C. Krug, E. B. O. da Rosa, C. Driemeier, I. J. R. Baumvol, and R. P. Pezzi, Appl. Phys. Lett. **92**, 252909 (2008).
[11] X. Zhu, H. D. Lee, T. Feng, A. C. Ahyi, D. Mastrogiovanni, A. Wan, E. Garfunkel, J. R. Williams, T. Gustafsson, and L. C. Feldman, Appl. Phys. Lett. **97**, 071908 (2010).
[12] C. Radtke, I. J. R. Baumvol, B. C. Ferrera, F. C. Stedile, Appl. Phys. Lett. **85**, 3402 (2004).
[13] G. V. Soares, C. Radtke, I. J. R. Baumvol, and F. C. Stedile, Appl. Phys. Lett. **88**, 041901 (2006).
[14] E. Pitthan, S. A. Corrêa, R. Palmieri, G. V. Soares, H. I. Boudinov, and F. C. Stedile, Electrochem. Solid-State Lett. **14**, H368 (2011).
[15] I. J. R. Baumvol, C. Krug, F. C. Stedile, F. Gorris, and W. H. Schulte, Phys. Rev. B **60**, 1492 (1999).
[16] A. Koh, A. Kestle, C. Wright, S. P. Wilks, P. A. Mawby, and W. R. Bowen, Appl. Surf. Sci. **174**, 210 (2001).

Reuse of AIP Publishing content is subject to the terms at: https://publishing.aip.org/authors/rights-and-permissions. Download to IP: 200.130.19.173 On: Wed, 20 Apr 2016 19:01:00

[17] M. Yoshikawa, S. Ogawa, K. Inoue, H. Seki, Y. Tanahashi, H. Sako, Y. Nanen, M. Kato, and T. Kimoto, Appl. Phys. Lett. **100**, 082105 (2012).
[18] V. V. Afanas'ev, A. Stesmans, and C. I. Harris, Mater. Sci. Forum **264–268**, 857 (1998).
[19] S. A. Corrêa, C. Radtke, G. V. Soares, I. J. R. Baumvol, C. Krug, and F. C. Stedile, Electrochem. Solid-State Lett. **11**, H258 (2008).
[20] S. Dhar, O. Seitz, M. D. Halls, S. Choi, Y. J. Chabal, and L. C. Feldman, J. Am. Chem. Soc. **131**, 16808 (2009).
[21] C. Önebby and C. G. Pantano, J. Vac. Sci. Technol. A **15**, 1597 (1997).
[22] Q. Zhu, L. Huang, W. Li, S. Li, and D. Wang, Appl. Phys. Lett. **99**, 082102 (2011).
[23] R. Palmieri, C. Radtke, H. Boudinov, and E. F. da Silva, Jr., Appl. Phys. Lett. **95**, 113504 (2009).
[24] W. Kern and D. S. Puotinem, RCA Rev. **31**, 187 (1970).
[25] I. J. R. Baumvol, Surf. Sci. Rep. **36**, 1 (1999).
[26] E. Pitthan, S. A. Corrêa, C. Radtke, G. V. Soares, and F. C. Stedile, BR patent 0260441 (2012).
[27] C. Driemeier, L. Miotti, R. P. Pezzi, K. P. Bastos, and I. J. R. Baumvol, Nucl. Instrum. Methods Phys. Res. B **249**, 278 (2006).
[28] B. E. Deal and A. S. Grove, J. Appl. Phys. **36**, 3770 (1965).
[29] E. A. Ray, J. Rozen, S. Dhar, L. C. Feldman, and J. R. Williams, J. Appl. Phys. **103**, 023522 (2008).
[30] H. Z. Massoud, J. D. Plummer, and E. A. Irene, J. Electrochem. Soc. **132**, 2685 (1985).
[31] K. Kouda, Y. Hijikata, S. Yagi, H. Yaguchi, and S. Yoshida, J. Appl. Phys. **112**, 024502 (2012).
[32] E. Szilágyi, P. Petrik, T. Lohner, A. A. Koós, M. Fried, and G. Battistig, J. Appl. Phys. **104**, 014903 (2008).
[33] M. Noborio, J. Suda, S. Beljakowa, M. Krieger, and T. Kimoto, Phys. Status Solidi A **206**, 2374 (2009).
[34] H. Watanabe, T. Hosoi, T. Kirino, Y. Kagei, Y. Uenishi, A. Chanthaphan, A. Yoshigoe, Y. Teraoka, and T. Shimura, Appl. Phys. Lett. **99**, 021907 (2011).
[35] S. K. Gupta, A. Azam, and J. Akhtar, Pramana, J. Phys. **76**, 165 (2011).
[36] E. Pitthan, R. Palmieri, S. A. Corrêa, G. V. Soares, H. I. Boudinov, and F. C. Stedile, ECS Solid-State Lett. **2**, P8 (2013).
[37] A. Pérez-Tomás, M. Lodzinski, O. J. Guy, M. R. Jennings, M. Placidi, J. Llobet, P. M. Gammon, M. C. Davis, J. A. Covington, S. E. Burrows, and P. A. Mawby, Appl. Phys. Lett. **94**, 103510 (2009).
[38] C. Kim, J. H. Moon, J. H. Yim, D. H. Lee, J. H. Lee, H. H. Lee, and H. J. Kim, Appl. Phys. Lett. **100**, 082112 (2012).
[39] Y. Ebihara, K. Chokawa, S. Kato, K. Kamiya, and K. Shiraishi, Appl. Phys. Lett. **100**, 212110 (2012).

Reuse of AIP Publishing content is subject to the terms at: https://publishing.aip.org/authors/rights-and-permissions. Download to IP: 200.130.19.173 On: Wed, 20 Apr 2016 19:01:00